

MASS BALANCE OF MARTIAN POLAR ICE FROM BAYESIAN FIT TO TROUGH MIGRATION PATHS. K. Izquierdo¹ (kig@purdue.edu), A. M. Bramson¹, T. McClintock², and K. Laferriere¹

¹Purdue University, EAPS, West Lafayette, IN, 47907 ²Cerebral Inc., San Francisco, CA.

Introduction: The ice mass balance of the North Polar Layered Deposits (NPLD) of Mars is currently unknown. The NPLD, pictured in Figure 1a, could be net accumulating or ablating. The insolation and corresponding stability of volatiles over the past millions of years have been affected by changes in obliquity of the planet in the range of 15° to 30° [1] making Mars' climate history complex. The record of present and past locations of surface depressions (i.e., troughs; Figure 1b) on the NPLD, however, help us constrain the past ice accumulation and sublimation rates. The past locations of these troughs are inferred from the location of discontinuities in the subsurface stratigraphy of the ice detected by the Shallow Radar (SHARAD) instrument onboard the Mars Reconnaissance Orbiter (Figure 2a) [2, 3].

In this work, we aim to constrain the mass balance of a local region of the NPLD by finding the accumulation and sublimation rates that generate the best fit to the trough migration paths (TMPs) of two adjacent troughs. Figure 1b shows the present location of the two troughs selected for this study. We build upon previous work [4] and constrain relevant mass balance conditions with a more complete and robust exploration of the climate parameter space.

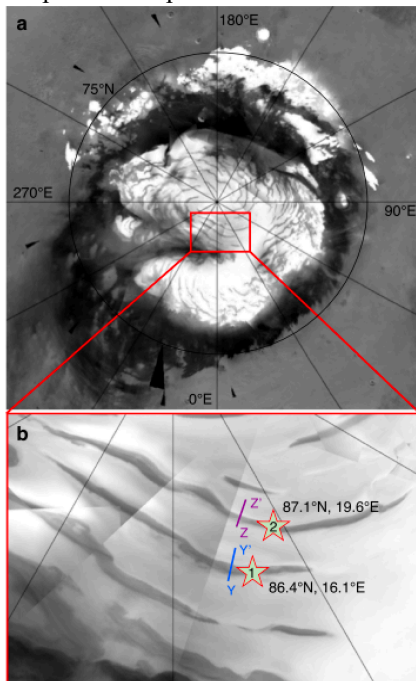


Figure 1: Mars Orbiter Camera mosaic showing the location of the troughs studied in this work. a) North polar ice cap. b) Zoom in to troughs 1 and 2. Modified from [4].

Methods: As in [4], we simplified the relationship between climate and migration of the troughs to generate synthetic trough migration paths. We assume the vertical displacement of the trough (y) per time is equal to the ice accumulation rate (A): $dy/dt = A$. We assume the horizontal displacement (x) per time is a function of the sublimation rate (R), slope of the trough (s), and A : $dx/dt = R + A \cos(s)/\sin(s)$ (Figure 2b). We construct a pool of candidate accumulation and sublimation submodels with varying number of parameters (n). We use a Markov chain Monte Carlo (MCMC) search for each trough to find the best fitting parameters as well as uncertainties of A and R . We constrain these parameters based on the fit of the synthetic TMP that they generate to the corresponding observed TMP obtained from SHARAD radargrams [4].

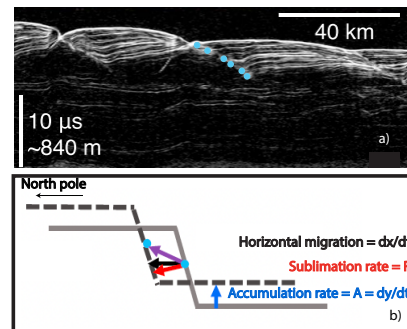


Figure 2: Trough migration model. a) Example of 2-D SHARAD radargram with blue dots showing an observed TMP. b) Schematic of how sublimation and accumulation result in vertical and horizontal migration. Modified from [4].

The candidate accumulation rate submodels are functions of local insolation with time $A(I(t))$ or obliquity of Mars with time $A(O(t))$. A can vary with $I(t)$ or $O(t)$ in a linear, quadratic, cubic or power law way. The candidate sublimation rate submodels $R(L(t), t)$ are functions of a protective dust layer ("lag") of thickness $L(t)$ that reduces sublimation compared to bare surface ice. A look-up table of sublimation rates for different lag thicknesses were calculated using a previously developed thermal model [4]. We test models of the lag thickness $L(t)$ being constant, linear, quadratic, cubic or following a power law with time. We combine each accumulation submodel with each sublimation submodels to create 80 candidate climate models for each trough.

We use the Emcee hammer Python module to construct an MCMC algorithm to find the posterior probability of the parameter values for each candidate

model according to Bayes' theorem. We run $4n$ chains with different, randomly chosen initial conditions for each model. At each iteration of the chain, the TMP produced by a randomly chosen set of parameter values is compared with the observed TMP data, and the parameter values which have a higher likelihood (l) are kept as part of the output ensemble. The likelihood is a function of the least squares misfit between synthetic and observed TMP, the number of data points and their uncertainty. After convergence is achieved, we obtain an ensemble of models with good fit to the observed TMP and from which best-fitting parameters and variations of those parameters are obtained. Finally, we select the climate model having the highest Bayesian Information Criterion (BIC) as a best representation of the accumulation and sublimation rates in the last five million years (the period of time tested here).

Results: The most representative climate model of Trough 1 is the one where the ice accumulation rate varies with obliquity in a cubic way $A(O(t)) = \alpha O(t)^3 + \beta O(t)^2 + \gamma O(t)$ and the lag thickness varies in a quadratic way $L(t) = \alpha_l t^2 + \beta_l t + \gamma_l$. The cubic obliquity submodel is also the best representation of the accumulation rates for Trough 2 while the best lag thickness submodel is the cubic one.

Figure 3 shows the excellent fit between the TMPs of the ensemble models, output of the MCMC, and the observed TMP, validating the ability of the inferred accumulation and sublimation parameters to reproduce the observations. Figure 3 also shows the corresponding modeled age of locations along the TMP observations, with the deepest points representing the oldest points recorded by the TMP (i.e. initiation). The distribution of ages on the right panel show that Trough 1 initiated 4.2 Mya while Trough 2 initiated 4.1 Mya. The ages are almost two times older than previously estimated [e.g., 4] and what is expected based on the current leading hypothesis of NPLD age [5].

Figure 4 shows the accumulation rates with time $A(O(t))$ of troughs 1 and 2 using the corresponding most representative climate model. Different colors show values of chains with different initial conditions. Accumulation rates are on the order of millimeters per year, consistent with the accumulation rates found in [4]. Figure 4 also shows the sublimation rates $R(L(t), t)$ of trough 1 and 2. The range of R values for the most recent 4 My are slightly higher than those in [4], while the values between 4 and 5 My are not well constrained and vary between all allowable values of 0 to 250 mm/y.

Discussion and conclusion: The synthetic TMPs of Trough 1 and 2 show how the main climate parameters (A and R) controlling the TMPs vary with time for the last 5 My. They have an excellent fit to the observed

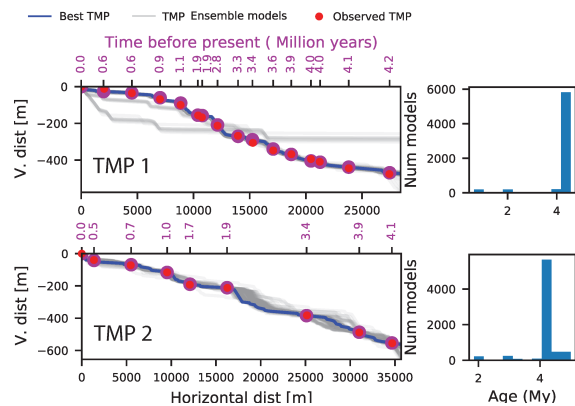


Figure 3: Comparison of TMPs of output climate models (grey lines) and best fit synthetic TMP (navy blue line) to the observed TMP (red dots) with the corresponding distribution of ages for each trough.

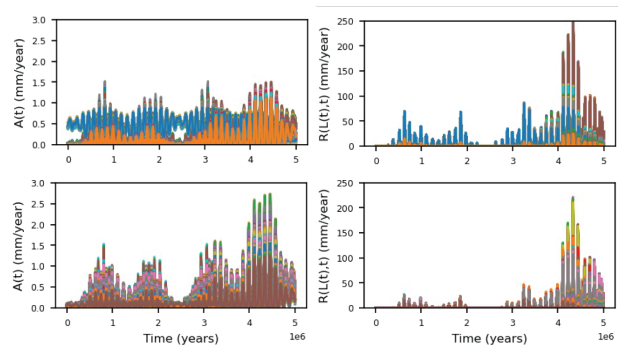


Figure 4: Inferred accumulation and sublimation rates for the last 5 My. Different colors correspond to different initial conditions of the MCMC.

TMPs and have accumulation rates in the same order of magnitude than previous work while sublimation rates and trough ages are higher. We propose that the accumulation and sublimation rates shown in Figure 4 are representative of the rates in the area surrounding trough 1 and 2 and that the Bayesian approach and exploration of the parameter space using a MCMC algorithm provides a better insight into how tight or loose are the constraints of A and R with time. In the future we plan to expand this work to more troughs in the NPLD to investigate further constraints on the spatial allocation of sublimated ice volumes (local, regional), which would provide a more complete view of the volatile mass balance of the NPLD.

References: [1] Laskar, J. et al. (2004) *Icarus*, 170, 343-364. [2] Smith, I., Holt, J. (2010) *Nature*, 465, 450-453. [3] Smith, I. & Holt, J. (2015) *JGR Planets* 120, 362-387. [4] Bramson, A. M. et al. (2019) *JGR Planets*, 124, 1020-1043. [5] Levrard B. et al. (2007) *JGR Planets*, 112, E06012.